PHOTOSYNTHETICA 48 (4): 596-609, 2010

Modelling photosynthetic photon flux density and maximum potential gross photosynthesis

R.J. RITCHIE

Faculty of Technology and Environment, Prince Songkla University – Phuket, Thailand 83120

Abstract

Irradiance data software developed by the NREL Solar Radiation Laboratory (Simple Model of Atmospheric Radiative Transfer of Sunshine, *SMARTS*) has been used for modelling photosynthesis. Spectra and total irradiance were expressed in terms of quanta [mol m^{-2} s^{-1}, photosynthetic photon flux density, PPFD (400–700 nm)]. Using the *SMARTS* software it is possible to (*1*) calculate the solar spectrum for a planar surface for any given solar elevation angle, allowing for the attenuating effects of the atmosphere on extraterrestrial irradiance at each wavelength in the 400–700 nm range and for the thickness of atmosphere the light must pass through during the course of a day, (*2*) calculate PPFD *vs.* solar time for any latitude and date and (*3*) estimate total daily irradiance for any latitude and date and hence calculate the total photon irradiance for a whole year or for a growing season. Models of photosynthetic activity *vs.* PPFD are discussed. Gross photosynthesis (P_g) *vs.* photosynthetic photon flux density (PPFD) (P_g *vs.* I) characteristics of single leaves compared to that of a canopy of leaves are different. It is shown that that the optimum irradiance for a leaf (I_{opt}) is the half-saturation irradiance for a battery of leaves in series. A C_3 plant, with leaves having an optimum photosynthetic rate at 700 μmol m^{-2} s^{-1} PPFD, was used as a realistic worked example. The model gives good estimates of gross photosynthesis (P_g) for a given date and latitude. Seasonal and annual estimates of P_g can be made. Taking cloudiness into account, the model predicts maximum P_g rates of about 10 g(C) m^{-2} d^{-1}, which is close to the maximum reported P_g experimental measurements.

Additional keywords: global models; gross photosynthesis; irradiance; light saturation curves; modelling; photoinhibition; photosynthetically active radiation; photosynthetic photon flux density; primary productivity.

Introduction

For most physical applications and in climatology solar energy is given in W m^{-2}; however, in photosynthetic applications, because of the quantum nature of the light reactions of photosynthesis, biologists are more interested in irradiance presented as photosynthetically active radiation (PAR) in units of mol m^{-2} s^{-1} (McCree 1973). The unambiguous name for PAR expressed in quantum terms is photosynthetic photon flux density (PPFD).

For a given wavelength of monochromatic light irradiance in terms of mol m^{-2} s^{-1} and W m^{-2} can be interconverted using the Planck equation:

$$P = \frac{N_A h n c}{\lambda}$$

or solving for n,

$$n = \frac{P\lambda}{N_A h c} \quad (1)$$

where P is the electromagnetic power delivered, expressed on a surface area basis (W m^{-2}), N_A is the Avogadro constant (6.0221367×10^{23} mol^{-1}), n is the

Received 25 March 2010, *accepted* 15 October 2010.
Present address: School of Biological Sciences A-08, The University of Sydney, NSW 2006, Australia.
Phone: +61 9351 4475, fax: +61 2 9351 4119, e mail: rrit3143@usyd.edu.au
Abbreviations: Chl – chlorophyll; ETI – extraterrestrial irradiance; ETR – electron transport rate; I – irradiance PPFD; I_d – daily irradiance PPFD, P_g – gross photosynthesis, PAR – photosynthetically active radiation, PPFD – photosynthetic photon flux density, PS – photosystem; *SMARTS* – Simple Model of Atmospheric Radiative Transfer of Sunshine; α_p – photosynthetic efficiency.
Acknowledgements: The author wishes to thank Dr John W. Runcie (University of Sydney), Emeritus Prof Tony Larkum and Mr Mark Curran (ret.) (University of Sydney) for their interest in this study and helpful comments on the paper. I especially wish to thank Dr Christian Gueymard for help in using the *SMARTS* software (NREL and Solar Consulting Services http:// www.SolarConsultingServices.com). This project was funded by an Endeavour Executive Award to the author (N° 1324_2009, Dept of Education and Training, Commonwealth of Australia).

number of moles of quanta per second on a surface area basis (mol m^{-2} s^{-1}), h is Planck's constant (6.6260755 × 10^{-34} J s), *c* is the speed of light in vacuum (2.99792458 × 10^{8} m s^{-1}), λ is the wavelength (m).

Unless the wavelength is specified it is not possible to interconvert PAR irradiance expressed in W m^{-2} and PPFD in mol m^{-2} s^{-1}. One mole of quanta is sometimes called one einstein but is not an official SI unit. For some types of light source there are approximate values for interconversion of PAR (400–700 nm) expressed in various units (Gensler 1984) but care needs to be taken in their use.

Very reliable extraterrestrial spectra of the sun have now been published (Gueymard *et al.* 2002, Reference Solar Spectral Irradiance 2003). Dr. C. Gueymard developed the *SMARTS* software (*SMARTS 2009*, http://www.nrel.gov/rrdc/smarts/) to model solar radiation reaching the earth's surface (Gueymard 1995, Gueymard 2001, *SMARTS 2009*). The NREL Solar Radiation Laboratory (http://www.nrel.gov/) hosts the *SMARTS* webpage and has developed the *Excel* interface.

Four properties of photosynthesis are often misunderstood when attempts are made to estimate potential primary productivity from irradiance data. These are; the quantum nature of the photosynthetic mechanism imposes a strict upper limit on carbon fixation rates, only part of the PPFD spectrum (400–700 nm) is actually used in photosynthesis and the photosynthetic mechanism, like most biochemical processes, is not only saturable but in addition substantial photoinhibition can occur at high irradiances.

In the present study I have developed a minimal model of photosynthesis based on accurate modelling of irradiance in quantum units. Using the *SMARTS* software (Gueymard 1995, Gueymard 2001, *SMARTS 2008*) and the NREL: Solar Position Calculators: SOLPOS it is possible to calculate irradiance at any latitude and solar elevation angle (corrected for refraction) over the period of a day for a given date. Numerical integration methods can then be used to calculate daily and yearly irradiances for a given latitude. Given a realistic model of photosynthesis that takes photoinhibition into account and allows for only part of the photosynthetically active radiation spectrum (400–700 nm) being actually useable for photosynthesis, it is possible to make realistic estimates of primary productivity for a given latitude and time of year. The models developed here are deliberately as simple and general as possible but take advantage of better irradiance data (Gueymard 1995, Gueymard 2001, NREL Solar Radiation Laboratory 2008, *SMARTS 2009*) and a better model of photosynthesis *vs.* irradiance.

Theory: development of a model of gross photosynthesis

Fig. 1 shows that plots of PPFD *vs.* wavelength, even for the sun's extraterrestrial spectrum, are not the smooth curves expected from a black body with a colour temperature of about 5,770 K. There are substantial absorption bands arising from the presence of elements in the chromosphere of the sun, in particular near 450 nm. The solar spectrum which reaches the ground is considerably modified by passing through the atmosphere (plotted in Fig. 1 as total irradiance upon a flat horizontal surface, global horizontal irradiance – total diffuse and direct sunlight as defined in the *SMARTS* software described in the Methods). Furthermore, the atmosphere does not behave as a simple neutral density filter, for example there is a strong absorption band at 687–698 nm and there is a general trend for absorption/scattering to be greatest for blue light and for the degree of absorption to decrease towards the red end of the spectrum. This effect is more pronounced for diffuse horizontal irradiance (skylight, as defined in the *SMARTS* software) than for direct sunlight (direct normal irradiance, as would be measured with a detector pointed directly at the sun) and global horizontal irradiance.

The overall photosynthetic reaction for C_3 photosynthesis (Larkum *et al.* 2003, Miller 2006, Falkowski and Raven 2007) is:

$$12H_2O + 6CO_2 + 54 \text{ photons } (hc/\lambda) \rightarrow C_6H_{12}O_6 + 6H_2O + 6O_2 \quad (2)$$

or expressed in the simplest ratios,

$$2H_2O + CO_2 + 9 \text{ photons } (hc/\lambda) \rightarrow (CH_2O)_n + H_2O + O_2$$

The theoretical efficiency of photosynthesis based upon the energy in 54 moles of photons with a wavelength of 680 nm (the red peak of Chl *a in vivo*) (Planck equation) and the energy required to synthesise one mole of glucose (2,803 kJ mol^{-1}) is about 29.5%. This upper limit for photosynthetic efficiency is often incorrectly thought to show that there is great room for improvement in the photosynthetic efficiency of plants growing in sunlight. Some of the reasons why this is an incorrect inference are:

(*1*) It is not possible for oxygenic photosynthesis to function with less than 9 photons per mole of carbon fixed: even 8 photons of red light will not provide enough ATP and NADPH+H^+ to fix one CO_2 molecule using the Calvin cycle (Larkum *et al.* 2003, Miller 2006, Falkowski and Raven 2007).

(*2*) 9 photons of blue light (Chl *a* peak ≈ 440 nm) cannot fix any more carbon than 9 photons of red light at 680 nm even though the blue photons have 680/440 or 54.5% more energy. This is why photosynthetic calculations should always use quantum units rather than radiometric units (W m^{-2}).

(*3*) Not all photons between 400 and 700 nm wavelengths are equally useable in photosynthesis. The

light harvesting by photosynthetic pigments and the quantum efficiency of photons actually absorbed varies considerably at different wavelengths. That is after all why leaves appear green in colour. For green algae and vascular plants containing Chl *a* and *b* (Larkum *et al.* 2003, Miller 2006, Falkowski and Raven 2007) in terms of the proportion of photons used for photosynthesis, the efficiency of the use of photons for photosynthesis is high near the *in vivo* blue and red absorption peaks of chlorophyll (Chl) *a* (440 & 680 nm respectively) but very low for green light (550 nm). The solar spectrum at wavelengths less than 425 nm is very depleted, particularly at ground level (Fig. 1) and so far-blue and violet light would contribute very little to total photosynthesis. Xanthophylls and carotenoids are accessory photosynthetic pigments, which absorb energy and transfer energy to the photoreaction centres of photosystems (PS) I and II. They absorb light at wavelengths from about 450 to 500 nm and efficiently transfer absorbed energy to PSI and PSII. These pigments provide an extension of the window of solar radiation useable for photosynthesis.

Based upon classical action spectra of photosynthesis (photosynthesis *vs.* wavelength of photons corrected to allow for the quantum nature of light) (McCree 1972, Kyewalyanga *et al.* 1997, Larkum *et al.* 2003, Miller 2006, Falkowski and Raven 2007), an estimate of light actually used for photosynthesis would be the sum of irradiance from 425 to 500 nm plus irradiance from 640 to 700 nm, allowing for the actual quantum efficiency at different wavelengths. Thus, an *optimistic* estimate of photosynthetically useable irradiance (I_{PUR}) is;

$$I_{PUR} \approx 0.668 \times \int_{425}^{500} I_\lambda \, d\lambda + 0.819 \times \int_{640}^{700} I_\lambda \, d\lambda \qquad (3)$$

where the constant 0.668 is the average quantum efficiency for blue light (425–500 nm) and 0.819 is the average quantum efficiency for red light (640–700 nm) based on polynomial interpolation of the data of McCree (1972) for a variety of crop plants. For full sunlight on earth, at the equatorial equinox, the PPFD is about 2,220 μmol m^{-2} s^{-1} but only 34.6% of the total irradiance (767 μmol m^{-2} s^{-1}) could actually be used in photosynthesis by Chl *a*/*b*-type plants (calculated from Eq. 3 for the standard solar spectrum for a flat surface at equatorial equinox shown in Fig. 1). Action spectra for organisms containing accessory Chl *c* of various types (diatoms, dinoflagellates and other chromophytes and the zooxanthellae of corals and clams) are essentially similar to those found for Chl *a*/*b*–type organisms (green algae and vascular plants) (Neori *et al.* 1988, Kühl *et al.* 1995, Kyewalyanga *et al.* 1997). In the present study, sun/shade adaptation of plants under low irradiance conditions to utilise as much light as possible in the green-yellow-orange parts of the spectrum (500–640 nm) and the "package effect" arising from self-shading effects of chloroplasts and light-harvesting pigments (Jones 1992) have been neglected because most of the photosynthesis of a forest canopy occurs in the top layers exposed to high irradiance. The overall contribution to total photosynthesis of heavily shaded leaves in a canopy would be small and so any special adaptations of them to very low irradiance would have little effect on the total photosynthesis of the canopy. The finding that differences in the "package effect" were not large in tropical forest sun and shade plants (Lee *et al.* 1990), is also reassuring.

Higher plants and green algae (Hodges and Barber 1983, Finazzi *et al*. 2002, Iwai *et al*. 2010) are able to use State I/State II transitions to adjust their photosynthetic mechanism to ambient conditions without the synthesis of new photosystems and antennae complexes. Thus to some extent they are able to adjust their photosynthetic action spectra to continuously fit their ambient light regime.

Cyanobacteria (blue-green algae), rhodophytes (red algae), glaucocystophytes and cryptophytes have phycobiliproteins which harvest green and yellow light, at least under low-light conditions (Subramaniam *et al.* 1999). Such photoautotrophs have much more dramatic rapid photoadaptation effects than in vascular plants and green algae. Eq. 3 cannot be easily adapted to apply to such algae by simply inserting a term to take light absorbed by phycobiliproteins into account. It is difficult to estimate how much of the PPFD window is usefully absorbed by phycobiliproteins because cells containing these accessory pigments are able to photo-adapt very quickly by coupling or decoupling their phycobilisomes from their photosystems (Subramaniam *et al.* 1999). Thus, in low irradiances phycobilin-containing algae would be able to use most absorbed light in the PPFD spectrum (400–700 nm) with high quantum efficiency but under high light conditions the phycobiliproteins would be decoupled and the cells would have an action spectrum similar to that of green algae and vascular plants (Eq. 3) (Ploug *et al.* 1993). Thus although phycobilin pigmentation of cyanobacteria confers an advantage under very low irradiances (Raven *et al.* 2000, Falkowski and Raven, 2007), in an open-air algal production pond under full sunlight the phycobilins confer less energetic advantage, compared to a green alga than usually thought because under such conditions the phycobilins are largely decoupled (Ploug *et al.* 1993, Subramaniam *et al.* 1999).

Objections to applying Eq. 3 to all oxyphotoautrophs turn out to be less justifiable than they at first appear to be. Eq. 3 is not an unreasonable approximation for modelling total photosynthesis by any community of oxyphotoautotrophs provided that (*1*) irradiance is high and (*2*) they use Chl *a* as the primary photochemical pigment. A forest, a dense crop, a bank of corals, an algal bloom, a cyanobacterial production pond or an algal mat should all use no more than about 30–40% of incident PPFD. Eq. 3 does not apply to the exotic cyanobacterium, *Acaryochloris marina*, because it uses Chl *d* (not Chl *a*) as its primary electron acceptor and uses light outside the

400–700 nm range (Gloag *et al.* 2007, Ritchie 2008). Eq. 3 would also not apply to oxyphotoautotrophic bacteria which use the newly-discovered Chl *f*, which has a methanol solvent absorption peak at 706 nm (Chen *et al.* 2010).

Surface inhibition of photosynthesis is well known to limnologists and oceanographers: models of primary productivity of oceanic phytoplankton have included consideration of the saturation and photoinhibition properties of the photosynthetic mechanism at high irradiances for a very long time (Walsby 1997, Miller 2006, Falkowski and Raven 2007, Ritchie 2008). Such models have been applied to algal mats (Ploug *et al.* 1993). Nevertheless, light saturation and photoinhibition properties of the photosynthetic mechanism are often neglected in models estimating theoretical primary productivity from irradiance data (Posada *et al.* 2009). Asymptotically saturating curves (*e.g.*, Michaelis-Menten, exponential saturation, non-rectangular hyperbolae and Tanh) can be used for modelling the response of photosynthesis to irradiance but such models would appear to only apply to irradiances below where photoinhibition sets in (Friend 2001, Larkum *et al.* 2003, Miller 2006, Falkowski and Raven 2007, Myeni *et al.* 2007). The waiting-in-line equation ($y = x\ e^{-x}$) has been found to be a very good model for photosynthesis for suboptimal, optimal and supraoptimal irradiances for photosynthetic materials that can be considered as a surface; for example leaves, algal mats, algae filtered onto glass fibre disks and algal suspensions with a short light-path. Two forms suitable for modelling photosynthesis (Gloag *et al.* 2007, Ritchie 2008, Ritchie and Bunthawin 2010) are,

$$P_g = P_{max}\, k_w\, I e^{1-k_w I} \qquad (4a)$$

or in a form more easily handled in non-linear curve fitting procedures,

$$P_g = P_{max} \cdot \frac{I}{I_{opt}}\, e^{1-I/I_{opt}} \qquad (4b)$$

where P_g is gross photosynthesis measured as electron transport rate (ETR), O_2 evolution or CO_2 uptake, P_{max} is the maximum gross photosynthesis, k_w is the waiting-in-line scaling constant for the PPFD axis, I is the irradiance (μmol m^{-2} s^{-1} PPFD), and I_{opt} is the irradiance at which maximum photosynthesis takes place (optimum irradiance). For the waiting-in-line equation it can be shown that P_{max} occurs when $I = 1/k_w$.

The maximum photosynthetic efficiency (α_p) is the initial slope of the curve at $I = 0$ ($\alpha_p = P_{max}\, e\, k_w$). At very low light intensities photosynthesis is directly proportional to irradiance. The half-maximum photosynthesis ($P_{half\text{-}max}$) occurs at $0.23120 \times I_{opt}$ and photosynthesis is inhibited by 50% at $2.6734 \times I_{opt}$ (Ritchie 2008).

Eqs. 4a,b apply to a photosynthetic surface that is opaque. In reality, photosynthesis is carried out by layers of photosynthetic cells, for example the leaf canopy of forests, grasslands and crops, algal mats, and water columns containing phytoplankton. In a community of photosynthetic cells most cells are at least partially shaded by cells above them, affording partial protection from the photoinhibitory effects of excessive irradiance. Integrated forms of Eqs. 4a or 4b are therefore appropriate for estimating photosynthesis by a uniform but multi-layered community of photosynthetic units.

The amount of photosynthetically useable radiation (I_{PUR}) at a given depth (x) inside a translucent photosynthetic material should approximately obey Lamberts law (Friend 2001, Sušila *et al.* 2004);

$$I_x = I_0\, e^{-k_i x} \qquad (5)$$

where x is the depth inside the photosynthetic material, k_i is the attenuation constant and I_0 is the PPFD at the surface of the photosynthetic entity.

For modelling purposes some broad generalisations need to be made about translucent photosynthetic materials (leaves of a canopy, algal mat or column of phytoplankton suspension). Generally the compensation point (where gross photosynthesis just balances respiration and hence net photosynthesis is zero) is at about 0.5% of full sunlight PPFD ($e^{-k_i x} \approx 0.005$) and so the compensation point is at about $0.005 \times 2\ 224 =$ 11.1 μmol m^{-2} s^{-1} (PPFD) (Raven *et al.* 2000). A compensation point between 4 and 20 μmol m^{-2} s^{-1} is a good generalisation over a wide range of photoautotrophs, except those adapted to very low irradiances which never experience full sunlight (Raven *et al.* 2000, Larkum *et al.* 2003, Falkowski and Raven 2007). The value of k_i will vary depending on the actual battery of photosynthetic units. Representative species in the Panamanian rainforest have a leaf area index of about 4 to 5 (Posada *et al.* 2009). On a broader scale, the leaf area index of the Amazonian rainforest averages 4.7 (Myeni *et al.* 2007) and so the k_i for such a closed canopy forest would be 1.127 calculated from Eq. 5 for 99.5% attenuation of light at ground level

It can be shown that taking Eq. 5, substituting into Eq. 4b and integrating over the depth (x) of the translucent photosynthetic material it is possible to estimate the total photosynthesis of a layer of photosynthetic cells that utilises all the useable light reaching the depth x in the photosynthetic material.

$$\sum P_g = \frac{P_{max}\, e}{k_i} \left(e^{-I_o e^{-k_i x}/I_{opt}} - e^{-I_o/I_{opt}}\right) \qquad (6a)$$

Eq. 6*a* is cumbersome and a more general simplified form is needed here. If we assume that a translucent layer of photosynthetic cells is thick enough to use virtually all of the useable light and hence $e^{-k_i x} \approx 0$ and so

$e^{-I_0 e - k_i x / I_{opt}} \rightarrow 1$, a good approximation is a simple exponential saturation curve (Eq. 6b) which is in form like the "big leaf" model used in forest studies (Friend 2001) but saturates very slowly. Note that the optimum irradiance for a leaf (I_{opt} from Eq. 4b) is the half saturation irradiance for a battery of leaves in series. The waiting-in-line model may be a better descriptor of photosynthesis *vs.* PPFD for individual leaves (Eq. 4b) than the asymptotic rectangular hyperbolae (Michaelis-Menten curve) often used in modelling photosynthesis (Thornley 1998, Friend 2001) but it turns out that a simple exponential saturation curve does describe photosynthesis *vs.* PPFD for a bank of leaves in series.

$$\Sigma P_g \approx \frac{P_{max}\ e}{k_i} (1 - e^{-I_o / I_{opt}}) \quad (6b)$$

Taking the photosynthetic equation (Eq. 2) and an estimate of useable PPFD (Eq. 3) it is possible to estimate P_g for a given irradiance regime. Leaves of terrestrial plants grown in full sunlight, such as clover and peas (C_3 plants), typically have a saturating rate of photosynthesis (I_{opt}) at about 700 µmol m^{-2} s^{-1} PPFD (White and Critchley 1999, Ritchie 2008). The quantity $P_{max} \times e/k_i$ can be taken as the theoretical maximum yield from photosynthesis for a given PPFD (P_{max} = 0.346/9 mol(C) mol^{-1}(photon) and an I_{opt} of 700 µmol m^{-2} s^{-1}. Substituting into Eq. 6b,

$$\sum P_g = \frac{0.84 \times 0.346 \times I \times (1 - e^{-I/700})}{9} =$$

$$= 0.03229 \times I \times (1 - e^{-I/700})$$

or,

$$\sum P_g = 0.3875 \times I \times (1 - e^{-I/700}) \quad (7)$$

where 9 photons are required to fix 1 carbon using C_3 photosynthesis (Eq. 2), 0.84 is the average leaf absorptance factor of Björkman and Demmig (1987) that is used in pulse amplitude modulation (PAM) fluorometers as a standard estimate of the proportion of PPFD irradiance that is actually absorbed by a photosynthetic surface (White and Critchley 1999, Gloag *et al.* 2007, Ritchie 2008), 34.6% of PPFD photons are actually potentially useable (Eq. 3), an optimum irradiance (I_{opt}) of 700 µmol m^{-2} s^{-1} PPFD, irradiance (I) is for the given time, date and latitude as PPFD.

Fig. 2 shows a plot of the Waiting-in-Line function for a P_{max} of 100% and an optimum irradiance (I_{opt}) of 700 µmol m^{-2} s^{-1} PPFD (k = 0.001429) where photosynthesis is expressed on a surface area basis (Eq. 4a) as well as for a translucent body absorbing and utilising all useable incident light (Eq. 7). A saturating irradiance of about 700 µmol m^{-2} s^{-1} PPFD would be representative for most C_3 vascular plants grown in full sunlight (Hodges and Barber 1983, White and Critchley 1999, Ritchie 2008). A photosynthetic surface with a photosynthetic optimum of 700 µmol m^{-2} s^{-1} PPFD would photosynthesise at half the maximum rate in an irradiance of only 161 µmol m^{-2} s^{-1} PPFD but would also be inhibited 50% at 1,871 µmol m^{-2} s^{-1} PPFD (Eqs. 4a,b). A multilayered photosynthetic material (canopy of leaves, algal mat or a water column containing phytoplankton) which consists of many layers of cells with P *vs.* I characteristics described by Eqs. (4a,b) would follow a simple exponential saturation curve (Eq. 7, Fig. 2). At least theoretically, a translucent photosynthetic surface, which absorbs all photosynthetically useable incident light, should exhibit an asymptotic saturation curve with no photoinhibition even though thin sections on the upper side will show photoinhibition at high irradiances.

Methods

Use of the *SMARTS 2.9.5* software: The *SMARTS 2.9.5* software (http://www.nrel.gov/rrdc/smarts/ NREL Solar Radiation Laboratory, Golden, CO, USA) was used to calculate PPFD spectra (400–700 nm) and total PPFD over time during daylight and daily total PPFD over the course of a year at a range of latitudes. The *SMARTS295* Users Manual PC and *SMARTS295i1.3* manuals were used as guides for configuring the software. The *SMARTS* software allows configurations to be checked for conflicts and stored as input files as *******_INP.txt. The software output is stored by the program as SMARTS295_OUT.txt and SMARTS295_EXT.txt. The SMARTS295_OUT.txt gives information on the conditions set for each run of the software and a summary of the output, but limited spectral information. The SMARTS295_EXT.txt provides complete spectral information for the spectral range specified (but can store no more than 64 spectra when *SMARTS* is implemented in Excel). These output files are overwritten on each run of the software and so have to be renamed for filing. Irradiance output terms used: direct normal irradiance—irradiance normal to the solar elevation angle (as would be measured by a collimated radiometer pointed directly at the sum), diffuse horizontal irradiance—scattered irradiance from the sky, global horizontal irradiance—total irradiance on a flat horizontal surface. Global horizontal irradiance is calculated by the *SMARTS* software but the calculated value is approximately the sum of the diffuse horizontal irradiance + sin (solar elevation angle) × direct normal irradiance.

The configurations used for the *SMARTS* software in the present study are shown in the Appendix. Default settings were used if appropriate. The U.S. Standard Atmosphere is the most commonly used atmospheric setting (Configuration Card 3). Other latitude-specific atmospheric settings are available as options in the

SMARTS software, *e.g*. tropical and arctic summer and arctic winter. As yet there are no standard settings for the Antarctic. The choice of atmospheric model has a noticeable effect on the irradiance at some specific wavelengths (*see* the spectral region 687–698 nm on Fig. 1) but its effect upon total PPFD (400–700 nm) is less than 0.2%. The default atmospheric CO_2 (370 ppmv) used by *SMARTS* (Configuration Card 7) is out-of-date: the estimated 2009 CE CO_2 level used in the present study was 389 ppmv based on data from the NOAA Earth System Research Laboratory (2009). The *SMARTS* default tilt is 37° (the standard tilt for solar panels) and the azimuth is set to 180° (facing directly south for the northern hemisphere) (Configuration Card 10a). For photosynthetic applications the tilt needs to be set to horizontal (zero tilt) and the azimuth value is not relevant for a flat horizontal surface. The appropriate spectral range (minimum 400 nm, maximum 700 nm) needs to be specified twice: on Configuration Cards 11 and 12.

Geometry for the calculation of atmospheric thickness: For the present study, values for the solar elevation angle (γ) corrected for atmospheric refraction and relative atmospheric mass (RAM) were obtained from the NREL solar radiation laboratory website (NREL solar radiation laboratory using SOLPOS). Standard settings were used except that all data was calculated for zero longitude (Greenwich). The solar elevation angle algorithms used by the SOLPOS software uses the Standard US atmosphere model to allow for the refractive properties of the atmosphere. 15-min intervals were chosen as suitable for the purposes of the present study. Solar angle data can also be accessed through the *SMARTS* software (Configuration Card 17). Differences arising from the choice of atmosphere models (Configuration Card 3) are only likely to be significant at low solar elevation angles where the irradiance on a horizontal flat surface would be low in any case.

Results

Fig. 1 shows the global horizontal irradiance spectra of sunlight expressed as μmol m^{-2} s^{-1} nm^{-1} from 400 to 700 nm calculated using the *SMARTS* software. Spectra are shown for extraterrestrial irradiance (ETI), the equator, Darwin, NT, Australia (12°28'S, 130°50'E), tropic of Cancer, 37°N and 55°N. The appropriate *SMARTS* atmosphere option was chosen for each of the above latitudes (tropical and mid-latitude). Atmospheric attenuation is more severe towards the blue end of the PPFD spectrum and so the maximum of the terrestrial spectrum is moved to longer wavelengths compared to the extraterrestrial spectrum. The lower the solar angle the more apparent this red-shift becomes because light has to pass through a thicker layer of atmosphere. Spectra were calculated for the March equinox for all latitudes except for Darwin where the September equinox was used. The emission spectrum of the sun (ETI), expressed as quanta (μmol m^{-2} s^{-1}), is different in appearance to when it is plotted in terms of energy (W m^{-2}). The maxima for solar emission are also different. The maximum for emitted photons is at 584 nm (9.1 μmol m^{-2} s^{-1} nm^{-1}).

Comparison of the ETI and spectra at a range of latitudes for the equinox clearly show that the attenuation properties of the atmosphere are quite different at different wavelengths (Fig. 1). The total irradiance for 400 to 700 nm can be summed: at the Equator, the total PPFD at noon at the equinoxes is 2,209 μmol m^{-2} s^{-1} (mean of March and September equinoxes), at 37°N the total PPFD onto a flat surface at the noon of the spring equinox is 1,240 μmol m^{-2} s^{-1}. Similar calculations could be made at any solar elevation angle using the *SMARTS* software (Gueymard 1995, Gueymard 2001, *SMARTS 2009*).

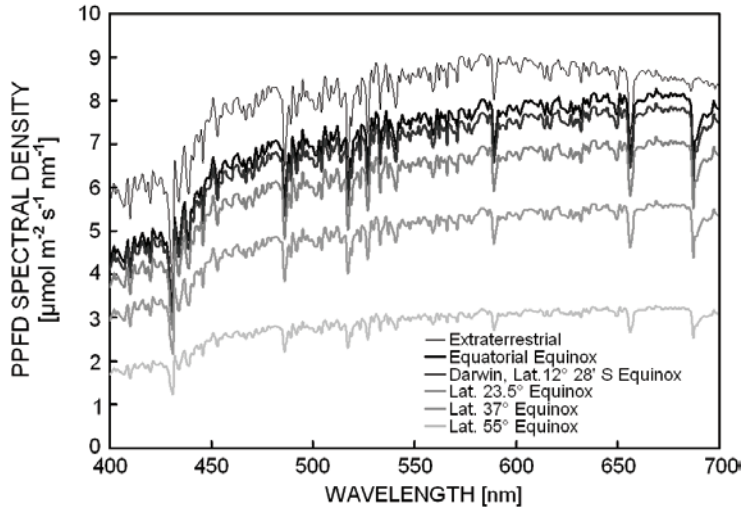

Fig. 1. Spectral density of PPFD through the atmosphere onto a planar surface. Solar spectra expressed in quantum terms for wavelengths from 400 to 700 nm (PPFD). The extraterrestrial spectrum (ETI) has strong absorption bands from elements in the chromosphere of the sun. In addition the atmosphere also has strong absorption bands. March equinox solar irradiance spectra are shown for the equator, tropic of Cancer (23°27'N), 37°N and 55°N and the September equinox values are shown for Darwin (12°28' S). Spectra were calculated using the *SMARTS* software (*SMARTS 2009*, Gueymard 1995, Gueymard 2001). Note the strong absorption bands near 487 nm and 687–698 nm which are within the blue and red absorption peaks of chlorophyll *a in vivo*.

Table 1. Theoretical primary productivity at various latitudes.

Latitude[o]	Solar latitude	Growing season	Daily PPFD [mol m^{-2} d^{-1}]	Daily carbon fixation [g(C) m^{-2} d^{-1}]	Total irradiance in growing season [mol m^{-2}]	Total carbon fixation for growing season [g(C) m^{-2}]
Tropic of Cancer 23°30'N	Summer solstice	All year (365 d)	64.2	21.8	18,615	6,136
	Equinox		52.7	17.6		
	Winter solstice		32.3	9.90		
Equator	Solstice	All year (365 d)	58.1	19.8	20,238	6,823
	Equinox		52.8	17.6		
Darwin (12°28'S)	Summer solstice	All year (365 d)	59.9	20.3	19,710	6,602
	Equinox		56.6	19.2		
	Winter solstice		43.4	13.9		
Tropic of Capricorn 23°30'S	Summer solstice	All year (365 d)	64.2	21.8	18,425	6,062
	Equinox		52.8	17.6		
	Winter solstice		33.3	9.90		
37°N	Summer solstice	7 months	66.2	22.3	12,208	4,031
	Equinox	01-Mar to 01-Oct	44.9	14.2		
	Winter solstice	(214 d)	20.2	4.98		
37°S	Summer solstice	7 months	66.3	22.3	11,915	3,927
	Equinox	01-Sep to 01-Apr	45.1	14.3		
	Winter solstice	(212 d)	20.2	4.98		
55°N	Summer solstice	5 months	64.7	20.8	8,130	2,533
	Equinox	01-May to 01-Oct	30.0	8.09		
	Winter solstice	(153 d)	5.27	0.606		
66.5°N	Summer solstice	4 months	63	18.6	5,649	1,589
	Equinox	01-Jun to 01-Oct	18.8	4.02		
	Winter solstice	(122 d)	0.172	0.0026		

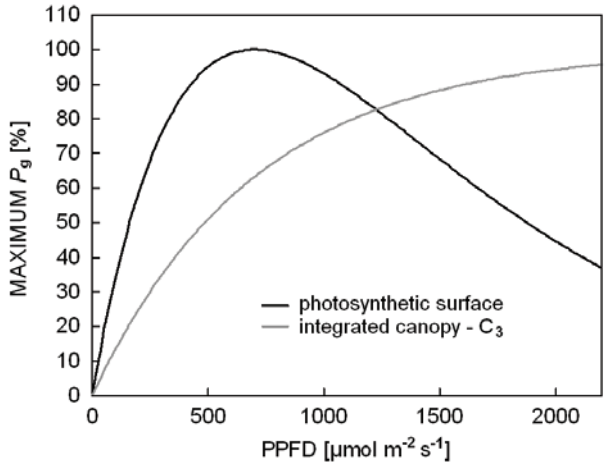

Fig. 2. Plot of the waiting-in-line function (Eqs. 4a,b) for an optimum irradiance of 700 µmol m^{-2} s^{-1} PPFD. The graph also shows a plot of total photosynthesis by a photosynthetic surface thick enough that it is able to utilize all available PPFD that is useable for photosynthesis (Eq. 7). Both equations have been scaled for P_{max} = 100%. P_g – gross photosynthesis; PPFD – photosynthetic photon flux density.

A table was compiled of global horizontal irradiance PPFD (µmol m^{-2} s^{-1}) on the ground for solar elevation angles from 0 to 90 degrees plus 23.5 and 66.5 degrees. A plot was made of PPFD *vs.* solar elevation angle. This curve was found to fit a 4th order polynomial very well (I = 0.00005643 γ^4 – 0.0132731 γ^3 + 0.805050 γ^2 + 18.417200 γ + 20.217710, r = – 0.99979, where γ is the solar elevation angle in degrees) and so total PPFD irradiance on flat horizontal ground can be calculated easily for any solar elevation angle by a simple formula. This could be used to calculate PPFD irradiance for any given latitude, time and date of a year given the solar elevation angle data from NREL Solar Radiation Laboratory (2008).

Fig. 3*A* shows diurnal light curves for irradiance on a flat planar surface for 37°N at summer solstice, winter solstice, the two equinoxes and for an arbitrary date 14-Aug-2009. The total daily PPFD irradiance (mol m^{-2}) can be calculated from the sum of the irradiance over the course of a day using the trapezium rule and numerical integration. The polynomial described above was used to calculate PPFD at 15-min intervals during the course of the day. The diurnal curve for 14-Aug-2009 lies between the light curve for the summer solstice and the equinox. If a similar plot is drawn for 37°S the photoperiods for the solstices and equinoxes are almost the same as for 37°N (there is a small effect due the small eccentricity of the earth's orbit). Total daily irradiance at the summer solstice (21-Jun-2009) was very high (66.3 mol m^{-2} d^{-1})

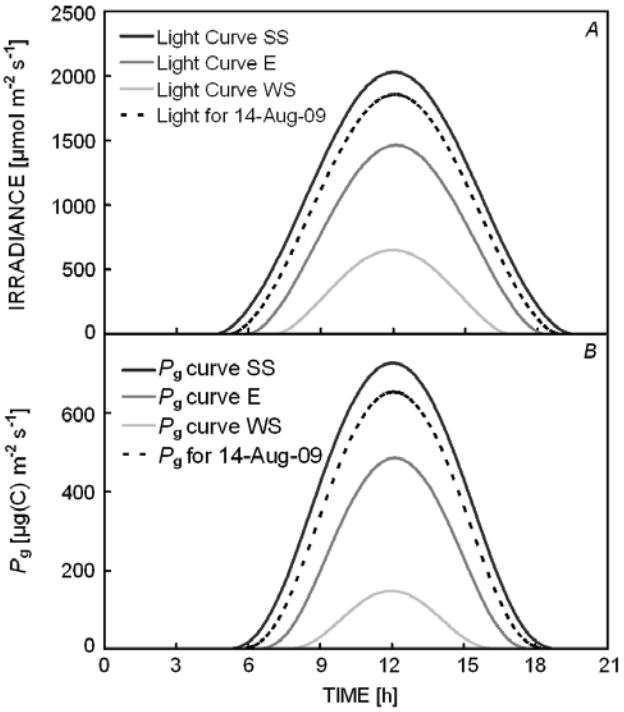

Fig. 3. *A*: Diurnal light curves for irradiance on a flat planar surface for 37° N at summer solstice, winter solstice, the two equinoxes and for an arbitrary date 14-Aug-2009. Irradiances are corrected for the thickness of the atmosphere through which the sunlight passes. The maximum noon PPFD is 2,130 µmol m^{-2} s^{-1} (66.3 mol m^{-2} d^{-1}) at the summer solstice (21-Jun-2009) and falls to 970 µmol m^{-2} s^{-1} (20.2 mol m^{-2} d^{-1}) for the winter solstice (21-Dec-2009). All mid-latitude diurnal light curves are similar in shape to Fig. 3*A*. *B*: The estimated diurnal gross photosynthesis (P_g) calculated using Eq. 7. In reality, the P_g value for the winter solstice would be negligible because it would be outside the growing season.

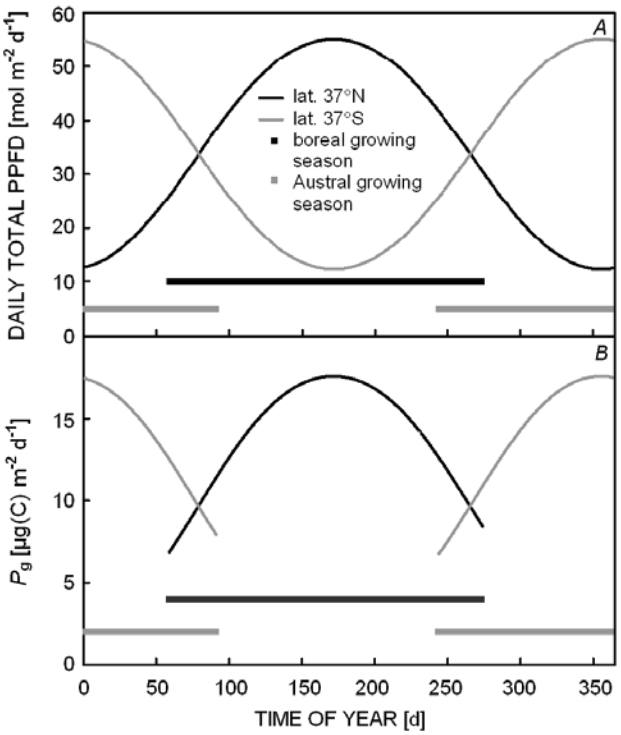

Fig. 4. *A*: Total daily gross photosynthesis (P_g) on a flat planar surface over a year for 37°N and S, calculated for each day of 2009. The curves are noticeably flattened in the winter months because of short daylight hours and low solar elevation angles. *B*: The estimated diurnal gross photosynthesis over a growing season from 01 March to 01 October calculated using the sum of P_g (estimated at 15-min intervals) over the course of each day.

because of the very long day length at that latitude at the summer solstice even though the maximum irradiance on the 21-Jun-2009 solstice (PPFD = 2,130 µmol m^{-2} s^{-1}) was less than the maximum found at the Equator (Table 1). Fig. 3*B* shows the estimated P_g in µg(C) m^{-2} s^{-1} (Eq. 7) over the course of a day. The daily photosynthesis curves are not the same shape as the irradiance curves because of the saturating response of photosynthesis to irradiance (Fig. 2).

Fig. 4*A* shows the daily irradiances for 37°N and S calculated for each day of 2009. The curves are noticeably flattened in the winter months because of shorter daylight hours and lower solar elevation angles. Total annual irradiance can be calculated by summation but for a mid-latitude situation it is not realistic to sum P_g over the entire year. For 37° latitude it would be reasonable to consider a growing season of about 7 months, starting from the start of the month of the spring equinox to the end of the month of the autumn equinox (Northern hemisphere; 1 March to 1 October and southern hemisphere; 1 September to 1 April). The total growing-season irradiances for 37°N are 12,208 mol m^{-2} (215 days) and 11,915 mol m^{-2} (212 days) for 37°S. Plots of daily P_g for days during the growing season are shown in Fig. 4*B*. Similar annual irradiance curves can be calculated for either hemisphere and for any latitude from data on solar elevation angle (Gueymard 1995, Gueymard 2001, NREL Solar Radiation Laboratory 2008, *SMARTS* 2009).

For graphs of daily irradiances for the tropics of Cancer and Capricorn and for the equator calculated daily over the course of a solar year please see the Supplementary material. Darwin (Northern Territory, Australia: 12°28'S) was included as an example of an intermediate site between the tropics of Capricorn and Cancer but not on the equator. The curves are similar for those found in mid-latitudes for the tropics of Cancer and Capricorn but at the equatorial maximum irradiance occurs twice a year at the equinoxes and is least when the sun is directly over the tropics of Cancer and Capricorn. The equator does not experience the maximum daily irradiance found on earth; these are experienced at the summer solstices at mid latitudes because of the longer day-length. Darwin is located almost half way between the equator and the tropic of Capricorn. The daily

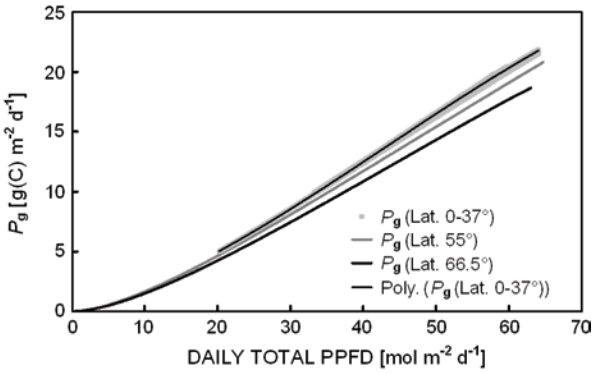

Fig. 5. Daily irradiances *vs.* gross photosynthesis (C_3) for the equator, tropics of Cancer or Capricorn (23°27' latitude) and 37°, 55°, and 66°27' latitudes. The curves for the equator and latitudes up to 37° overlap and can be collectively described by a single simple 3rd order polynomial of the form y = –0.00004574 x^3 + 0.00591451 x^2 + 0.148612 x where x is the total daily PPFD in mol m^{-2} d^{-1}, r = 0.9996.

irradiance at the equinoxes and the summer solstice are almost equal and are not the dates at which maximum irradiance occurs. Maximum irradiances (2,224 µmol m^{-2} s^{-1}; 59.6 mol m^{-2} d^{-1}) occur at midday on 16-Feb-2009 and 25-Oct-2009 when the sun past directly overhead at the latitude of Darwin. There is little variation in the day length over the year (about 11 to 13 h). Eq. 7 could be used to estimate P_g over the course of a day and hence estimate daily carbon fixation.

In the case of tropical environments, it is realistic to sum total irradiance over the year, because it is usually warm enough for plants to grow all year round. Table 1 shows that the total annual irradiances in the tropics are remarkably uniform: tropic of Cancer, 18,615 mol m^{-2}; equator, 20,238 mol m^{-2} and tropic of Capricorn, 18,425 mol m^{-2}, Darwin (12°28'S), 19710 mol m^{-2}. Darwin experiences a very high total annual irradiance even though it does not experience the highest daily irradiance on a global scale. Leaving aside water limitations, potential daily P_g would be expected to closely follow daily irradiance in tropical regions (*see* Supplementary material).

The large data sets of irradiance data and estimates of P_g used to prepare graphs of daily P_g *vs.* I_d can be used to plot estimated daily P_g *vs.* daily irradiance of C_3 plants (Fig. 5). The curves fit a simple 3rd order polynomial very well. Curves for latitudes from the equator to 37° overlap (37°N, tropic of Cancer, equator, Darwin, tropic of Capricorn, 37°S). For tropical and mid-latitudes a general relationship between daily PPFD irradiance and estimated P_g based on the present study is;

$$P_g = -0.00004574\ I_d^3 + 0.00591451\ I_d^2 + 0.148612\ I_d \quad (8)$$

where r = 0.9996.

Discussion

Use of the *SMARTS* software (Gueymard 1995, Gueymard 2001, *SMARTS 2009*) more easily allows comparisons between harvesting solar energy using solar panels and proposals to grow plants for production of biofuels. Much of the meteorological and climatology literature quotes PAR irradiance in W m^{-2}: the approximate conversion factor derived from the present study was 1 W m^{-2} PAR ≈ 4.556 µmol m^{-2} s^{-1} PPFD. This value was calculated by the author based upon a mean calculated from PPFD irradiance at solar elevation angles from 30 to 90° through the US Standard Atmosphere. This is within 1% of the conversion factor (4.6) given by Gensler (1984). My value is slightly lower than the value of 4.6 given by Gensler (1984) because there is a slight 'red shift' at low solar angles because blue light is more heavily absorbed/scattered than red light when passing through a thick layer of the earth's atmosphere.

The *SMARTS* software (Gueymard 1995, Gueymard 2001, *SMARTS 2009*) has been shown in the present study to useable for both northern and southern hemispheres. Calculations made in the present study agree very well with irradiance models developed by Walsby (1997) for total irradiances for given latitude but Walsby's models do not offer spectral information and irradiances were expressed in W m^{-2}.

Using a combination of data calculated using the *SMARTS* software and the solar elevation angle data from the NREL solar radiation laboratory website it is possible to calculate PPFD *vs.* solar time for any latitude and date allowing for the attenuating effects of the varying thicknesses of the atmosphere the incoming solar radiation passes through during the course of a day (relative atmospheric mass, RAM) (Fig. 3*A*). The model will not only be useful for modelling primary production from natural vegetation, crops and algal ponds for biofuel production but will lead to more realistic estimates of photosynthetic efficiency of plant communities in climatic and environmental studies. Estimates of total daily irradiance for any latitude and date, by numerical integration, makes it possible to calculate the maximum theoretical total irradiance for a whole year or for a growing season (Fig. 4*A*).

The photosynthetic model developed in the present study can be used to make estimates of theoretical maximum P_g for a given date, latitude and hemisphere, taking the saturation and optimum irradiance properties of C_3 photosynthesis into account (Eqs. 3, 4, and 6*b*; Table 1). Estimates of gross photosynthesis shown in Fig. 3*B*, 4*B*, and Table 1 are based upon a closed canopy of C_3 leaves able to use all useable light and having an optimum irradiance requirement of about 700 µmol m^{-2} s^{-1} (PPFD). Figs. 3*A,B* and Table 1 show that high rates of productivity are possible at mid-latitudes [up to about 22 g(C) m^{-2} d^{-1}]. However, winters at 37°N are

sufficiently cold to prevent significant photosynthesis during part of the year. Here I have assumed a growing season of about 7 months (01 March to 01 October). Annual gross photosynthesis could be no more than about 4.1 kg(C) m^{-2} y^{-1} or 41 tonnes per hectare per year (Figs. 4*A,B*; Table 1). Allowances for respiration outside the growing season would reduce annual net photosynthesis considerably from estimates of net photosynthesis made during the growing season.

Given optimal light and unlimited other resources it is possible to achieve annual gross photosynthetic rates of about 6.0 to 6.9 kg(C) m^{-2} y^{-1} or 60 to 69 t ha^{-1} $year^{-1}$ in the tropics in C_3 plants (Table 1, for examples of tropical irradiance curves see Supplementary material, Figs. 1S, 2S). Net production would be considerably lower because complete usage of available light can only be achieved by having a leaf area index much greater than unity. A large leaf area index implies a large biomass of leaves that perform minimal photosynthesis because they are usually in heavy shade but would make a large contribution to respiration, hence cutting down overall net photosynthesis. Leaf area index is finely regulated by plants because excess leaves are costly in terms of carbon for the plant to synthesise and to maintain.

Taking the primary production values for the tropics (Table 1) it is possible to calculate that the overall efficiency of gross photosynthesis reaches about 2.8% in terms of conversion of moles of PPFD quanta into moles of carbon (Eq. 8, Fig. 5). This agrees well with actual measurements in the laboratory (Richmond 1999, Falkowski and Raven 2007, Waltz 2009). Somewhat counter-intuitively Eq. 8 (daily total P_g *vs.* PPFD for tropical latitudes and 37°N, S) shows that the maximum photosynthetic efficiency of a canopy of C_3 leaves, absorbing all useable light, is maximal under the maximum daily irradiance found in the present study (67.8 mol m^{-2} d^{-1}; efficiency 2.8%) and falls to 2.1% at 20.7 mol m^{-2} d^{-1}. My estimates of maximum efficiency are less optimistic than Zhu *et al.* (2008) (≈ 4% for C_3 plants to 6% for C_4 plants) because mine were calculated on a quantum, rather than an energy basis, and because mine are based on total daily irradiance rather than optimum irradiance.

In high summer high latitudes such as 55°N and the Arctic Circle receive as much PPFD per day as the tropics but only for a short period of the year (Table 1). Some of the reasons why high productivity can be found in the short summers of very high latitudes on land and in oceanic systems are the combination of very long hours of daylight, hence minimal night-time respiratory losses during the growing season, combined with a lower maximum irradiance due to the low solar angle which lessens photoinhibition.

Calculations of irradiance calculated in the present study are of course for cloudless skies. Thus, any site on earth will receive considerably less irradiance than the maximum. Few data sets of actual PAR or PPFD measurements under natural conditions (rather than crude estimates derived from other measurements) are available and modelling PAR or PPFD under cloud cover is not straightforward (Rubio *et al.* 2005, Olofsson *et al.* 2007). Cloud cover approximately behaves in the 400–700 nm windows like a neutral density filter (they appear white or grey). Clouds also scatter light to create a diffuse light source. There is also an apparent "blue shift" in total irradiance because diffuse light from the blue celestial dome (diffuse horizontal irradiance) becomes a more significant contributor to total irradiance under cloudy conditions. The absorbance and light scattering properties of high cirrus, cumulus and nimbus clouds are different. The effects of clouds upon irradiance also differ with solar elevation angle; for example, the probability of a ray of sunlight passing through a cloud is less for high solar elevation angles than for low solar elevation angles. The degree of cloudiness and the type of cloud cover varies greatly with geographic location. Information on hours of sunshine and cloudiness can be found in the meteorological records and in the climatological literature and from satellite monitoring projects (*e.g.* Rossow and Duenas 2004, Reikard 2009) and on the worldwide web (for example for Australia: Climate graphs and maps-average daily sunshine hours: [http://www.bom.gov.au/climate/averages/climatology/sunshine_hours/sunhrs.html], worldwide: International Satellite Cloud Climatology project (ISCCP): [http://www.gewex.org/ isccp.html]). Meteorological measurements of irradiance are generally expressed in W m^{-2} (radiometric units measured using a pyranometer) and cover the near-UV, visible and near infrared wavelengths of light (full sunlight broadband or shortwave irradiance is about 1,100 W m^{-2} for a window of 300–4,000 nm) and so are not restricted to the PAR window (full sunlight global PAR irradiance is about 485 W m^{-2}). Since the absoption/scattering properties of clouds for infrared and PAR windows are so different, conversion factors for solar radiation reported as shortwave irradiance to PAR are only approximate and actual measurements of the conversion factor vary considerably (from 0.27 to 0.48) depending upon the actual meteorological conditions and solar angle (Rubio *et al.* 2005, Olofsson *et al.* 2007). Furthermore, meteorological data sets are often further processed in ways which restrict their usefulness for photosynthetic studies. For example, "hours of sunshine" is defined by the hours where the broadband irradiance is above 120 W m^{-2}. This is a relatively high value in photosynthetic terms, equivalent to about 220 μmol m^{-2} s^{-1} (PPFD) which is about 10% of full sunlight. Leaves of many C_3 plants growing in full sunlight would be capable of photosynthesis of more than half of the P_{max} under such conditions (Eqs. 4a,b).

Thus, zero "hours of sunshine" does not imply zero photosynthesis: substantial photosynthesis can occur on an overcast day registering zero "hours of sunshine". This

is quite the reverse of what a naïve understanding of the "hours of sunshine" statistic would lead one to believe. In the tropics, in the wet season, it is not unusual for days to be overcast in excess of 10 h per day. A diffuse-source PPFD of 220 μmol m^{-2} s^{-1} or about 5 to 8 mol m^{-2} d^{-1} would qualify as a cloudy day with "zero sunshine" but would provide enough photons to fix about 1 g(C) m^{-2} d^{-1} (Eq. 8): the actual figure would probably be higher because in the wet season some photoacclimation would be expected to the lower light conditions, there would be less photoinhibition, less photorespiration and a diffuse light source favours high photosynthesis (Friend 2001, Myeni *et al.* 2007, Posada *et al.* 2009). Primary production during tropical wet seasons and tropical high-altitude cloud forests, more or less permanently under cloud cover, are both very high and plants are photoacclimated to lower average irradiance than full sunlight and the leaf area index is adjusted accordingly (Myeni *et al.* 2007, Posada *et al.* 2009).

Cloudiness significantly affects potential photosynthesis. Darwin has a dry-monsoon climate and very high clear-sky irradiances. It would seem a good site for biofuel production. Clear-sky irradiances at the latitude of Darwin are very high over much of the year (Table 1) but cloud cover would have large effects during the hot wet-season (October to March). Using the Australian Meteorological Office data referred to above, during the winter drought day lengths are about 11 h but hours of sunshine are in excess of 9 h (zero cloud-cover) and so daily maximum gross photosynthetic rates would remain at about 11 g(C) m^{-2} d^{-1} (Table 1). During the wet season, daylight hours are about 13 hours but hours of sunshine average only 8 h per day and so maximum daily Gross Photosynthesis would be the sum of about 8 hours photosynthesis in full sunshine plus 5 hours under cloud or a total of about 13 g(C) m^{-2} d^{-1}. These maximum estimates of Gross Photosynthesis are close to the experimentally observed maximum primary productivity found in rainforests and crops [about 10 g(C) m^{-2} d^{-1}] even though productivity by terrestrial vascular plants is often water-limited, which causes stomatal closure, hence limiting CO_2 fixation (Taize and Zeiger 2002).

Very large amounts of time and money have been spent on the concept of using algal ponds or more conventional crops to produce biofuels (Richmond and Zhou 1999, Antoni *et al.* 2007, Grobbelaar 2007, Huntley and Redalje 2007, Waltz 2009). More detached assessments (Sheehan *et al.* 1998, Walker 2009, Larkum 2010) have concluded that they are unlikely to be viable. Walker (2009) points out that there seems to be a stubborn resistance to accepting the point that such schemes have little chance of being viable. Some carbon fixation rates claimed for algal production ponds [40 to 100 g(C) m^{-2} d^{-1}: Richmond and Zhou 1999, Waltz 2009] are well above the theoretical limits calculated in the present study for a photosynthetic organism (Eqs. 2, 3).

Some of the fundamental errors common in studies of the relationship between irradiance and photosynthesis and hence primary productivity are: (*1*) the simple fact that sunlight is a *dilute* energy source is not understood, (*2*) the quantum nature of the light reactions of photosynthesis is not appreciated, (*3*) only part of the so-called PPFD spectrum is actually used for photosynthesis, (*4*) the wrong solar irradiance units of measurement are used or (*5*) global horizontal irradiance PPFD solar irradiances for noon at the equator at equinox (≈2,220 μmol m^{-2} s^{-1}) are used where it is not appropriate to do so (solar elevation angle is neglected), (*6*) the saturable nature of the photosynthetic apparatus is not appreciated (Ritchie 2008) and (*7*) photosynthetic efficiency under natural lighting conditions is grossly overestimated because photosynthetic efficiencies calculated from the initial slope of P *vs.* I curves have been inappropriately used (Ritchie 2008). The *Excel* routines used in the present study are available from the author upon request.

References

Antoni, D., Zverlov, V.V., Schwarz, W.H.: Biofuels from microbes. – Appl. Microbiol. Biotechnol. **77**: 23-35, 2007.

Björkman, O., Demmig, B.: Photon yield of O_2 evolution and chlorophyll fluorescence characteristics at 77K among vascular plants of diverse origins. – Planta **170**: 489-504, 1987.

Chen, M., Schliep, M., Willows, R.D., Cai, Z.-L., Neilan, B.A., Scheer, H.: A red-shifted chlorophyll. – Science **329**: 1318-1319, 2010.

Falkowski, P.G., Raven, J.A.: Aquatic photosynthesis, 2nd Ed., Princeton Univ. Press, Princeton 2007.

Finazzi, G., Rappaport, F., Furia, A., Fleischmann, M., Rochaix, J-D., Zito, F., Forti, G.: Involvement of state transitions in the switch between linear and cyclic electron flow in *Chlamydomonas reinhardtii*. – EMBO Rep. **31**: 280-285, 2002.

Friend, A.D.: Modelling canopy CO_2 fluxes: are "big leaf" simplifications justified? – Global Ecol. Biogeogr. **10**: 603-619, 2001.

Gensler, W.G. (ed.): Advanced agricultural instrumentation. – In: Proc. NATO advanced Study Inst: Advanced Agricultural Instrumentation. Martinus Nijhoff Publ., Dordrecht 1984.

Gloag, R.S., Ritchie, R.J., Chen, M., Larkum, A.W.D., Quinnell, R.G.: Chromatic photoacclimation, photosynthetic electron transport and oxygen evolution in the Chlorophyll *d*-containing oxyphotobacterium *Acaryochloris marina* Miyashita. – BBA - Bioenergetics **1767**: 127-135, 2007.

Grobbelaar, J.U.: Photosynthetic characteristics of *Spirulina platensis* grown in commercial-scale open outdoor raceway ponds: what do the organisms tell us? – J. Appl. Phycol. **19**: 591-598, 2007.

Gueymard, C.: SMARTS, A Simple Model of the Atmospheric Radiative Transfer of Sunshine: Algorithms and Performance Assessment, Professional Paper FSEC-PF-270-95. – Florida Solar Energy Center, Cocoa 1995.

Gueymard, C.: Parameterized Transmittance Model for Direct Beam and Circumsolar Spectral Irradiance. – Sol. Energy **71**: 325-346, 2001.

Gueymard, C.A., Myers, D., Emery, K.: Proposed reference irradiance spectra for solar energy systems testing. – Sol. Energy **73**: 443-467, 2002.

Hodges, M., Barber J.: Photosynthetic adaptation of pea plants grown at different light intensities: State 1 – State 2 transitions and associated chlorophyll fluorescence changes. – Planta **157**: 166-173, 1983.

Huntley, M.E., Redalje, D.G.: CO_2 mitigation and renewable oil from photosynthetic microbes: a new appraisal. – Mitig. Adapt. Strategies Global Change **12**: 573-608, 2007.

Iwai, M., Takizawa, K., Tokutsu, R., Okamuro, A., Takahashi, Y., Minagawa, J.: Isolation of the elusive supercomplex that drives cyclic electron flow in photosynthesis. – Nature **464**: 1210-1214, 2010.

Jones, H.G.: Plants and Microclimate: A Quantitative Approach to Environmental Plant Physiology. 2nd Ed. – Cambridge Univ. Press, Cambridge 1992.

Kyewalyanga, M.N, Platt T., Sathyendranath S.: Estimation of the photosynthetic action spectrum: Implication for primary production models. – Mar. Ecol. Prog. Ser. **146**: 207-223, 1997.

Kühl, M., Cohen, Y., Dalsgaard, T., Jørgensen, B.B., Revsbech, N.P.: Microenvironment and photosynthesis of zooxanthellae in scleractinian corals studied with microsensors for 0_2, pH and light. – Mar. Ecol. Prog. Ser **117**:159-172, 1995.

Larkum, A.W.D.: Limitations and prospects of natural photosynthesis for bioenergy production. – Curr. Opin. Biotech. **21**: 271-276, 2010.

Larkum, A.W.D., Douglas, S.E., Raven, J.A. (ed.): Photosynthesis in Algae. – Kluwer Academic Publish., Dordrecht – Boston – London 2003.

Lee, D.W., Bone, R.A., Tarsis, S.L., Storch, D.: Correlates of leaf optical properties in tropical forest sun and extreme shade plants. – Amer. J. Bot. **77**: 370-380, 1990.

McCree, K.J.: The action spectrum, absorbance and quantum yield of photosynthesis in crop plants. – Agr. Meteorol. **9:** 191-216, 1972.

McCree, K.J.: The measurement of photosynthetically active radiation. – Sol. Energy **15:** 83-87, 1973.

Miller, C.B.: Biological Oceanography, – Blackwell Publ., Malden 2006.

Myeni, R.B., Yang W., Nemani, R.R. *et al*: Large seasonal swings in leaf area of Amazon rainforests. – Proc. Natl. Acad. Sci. USA **104:** 4820-4823, 2007.

Neori, A., Vernet, M., Holm-Hansen, O. and Haxo, F.T.: Comparison of chlorophyll far-red and red fluorescence excitation spectra with photosynthetic oxygen action spectra for photosystem II in algae. – Mar. Biol. Progr. Ser. **44**: 297-302, 1988.

NOAA Earth System Research Laboratory: Mauna Loa annual mean data. – http://www.esrl.noaa.gov/gmd/ccgg/trends [Accessed 15 November 2009].

NREL Solar Radiation Laboratory (2008): Solar position calculators (SOLPOS). – http://www.nrel.gov/midc/ srrl_bms/ [Accessed 01 October 2009].

Olofsson, P., Van Laake, P.E., Eklundh, L.: Estimation of absorbed PAR across Scandinavia from satellite measurements. Part I: Incident PAR. – Remote Sens. Environ. **110**: 252-261, 2007.

Ploug, H., Lassen, C. , Jørgensen, B.B.: Action spectra of microalgal photosynthesis and depth distribution of spectral scalar irradiance in a coastal marine sediment of Limfjorden, Denmark. – FEMS Microbiol. Ecol. **12**: 69-78, 1993.

Posada, J.M., Lechowicz, M.J., Kitajima, K.: Optimal photosynthetic use of light by tropical tree crowns achieved by adjustment of individual leaf angles and nitrogen content. – Ann. Bot. **103**: 795-805, 2009.

Raven, J.A., Kübler, J.E., Beardall J.: Put out the light, and then put out the light. – J. Mar. Bio Ass. U.K. **80**:1-25, 2000.

Reference Solar Spectral Irradiance: Air Mass 1.5 (2003) ASTM G173-03. – http://rredc.nrel.gov/solar/spectra/am1.5/ [Accessed 02 November 2008].

Richmond, A., Zou, N.: Efficient utilisation of high photon irradiance for mass production of photoautotrophic microorganisms. – J. Appl. Phycol. **11**: 123-127, 1999.

Reikard, G.: Predicting solar radiation at high resolutions: A comparison of time series forecasts. – Sol. Energy **83**: 342-349, 2009.

Ritchie, R.J.: Fitting light saturation curves measured using PAM fluorometry. – Photosynth. Res. **96**: 201-215, 2008.

Ritchie R.J., Bunthawin S.**:** The use of Pulse Amplitude Modulation (PAM) fluorometry to measure photosynthesis in a CAM orchid, *Dendrobium* ssp. *(D. 'Viravuth'* Pink). – Int. J. Plant Sci. **171**: 575-585, 2010.

Rubio, M.A., López, G., Tovar, J., Pozo, D., Batlles, F.J.: The use of satellite measurements to estimate photosynthetically active radiation. – Phys. Chem. Earth **30:** 159-164, 2005.

Rossow, W.B., Duenas, E.N.: The International Satellite Cloud Climatology Project (ISCCP) Web site. – Bull. Amer. Meteor. Soc. **85**: 167-172, 2004.

Sheehan, J., Dunahay, T., Benemann, J., Roessler, P.: A look back at the US Department of Energy's Aquatic Species Program: Biodiesel from Algae, NREL/TP-580-24190. NREL, Golden, Colorado, USA 1998. http: //www1.eere.energy.gov/biomass/pdfs/biodiesel_from_algae. pdf. [Accessed 03 January 2009].

Simple Model of Atmospheric Radiative Transfer of Sunshine (SMARTS) http://www.nrel.gov/rredc/smarts/ [Accessed 23/11/2009].

Subramaniam, A., Carpenter, E.J., Karentz, D., Falkowski, P.G.: Bio-optical properties of the marine diazotrophic cyanobacteria *Trichodesmium spp*. I. Absorption and photosynthetic action spectra. – Limnol. Oceanogr. **44**: 608-617, 1999.

Sušila, P., Lazár, D., Ilík, P., Tomek, P., Nauš, J.: The gradient of exciting radiation within a sample affects the relative height of steps in the fast chlorophyll *a* fluorescence rise. – Photosynthetica **42**: 161-172, 2004.

Taize, L., Zeiger, E.: Plant Physiology. 3rd Ed. Sinauer Associates, Sunderland 2002.

Thornley, J.H.M.: Dynamic model of leaf photosynthesis with acclimation to light and nitrogen. – Ann. Bot. **81**: 421-430, 1998.

Walker, D.A.: Biofuels, facts, fantasy and feasibility. – J. Appl. Phycol. **21**: 509-517, 2009.

Walsby, A.E.: Numerical integration of phytoplankton photosynthesis through time and depth in a water column. – New Phytol. **136**: 189-209, 1997.

Waltz, E.: Biotech's green gold? – Nature Biotechnol. **27**: 15-18, 2009.

White, A.J., Critchley, C.: Rapid light curves: A new fluorescence method to assess the state of the photosynthetic apparatus. – Photosynth. Res. **59**: 63-72, 1999.

Zhu, X.-G., Long, S.P., Ort, D.R.: What is the maximum efficiency with which photosynthesis can convert solar energy into biomass? – Curr. Opin. Biotech. **19**: 153-159, 2008.

Appendix: Configuration settings used for running *SMARTS 2.9.5* software

Card 1: Comments Enter a title name for *SMARTS* configuration.	**Card 10: Regional albedo (predominate within r = 10 km)** Selected vegetation: ***Grazing field (unfertilised)***
Card 2: Site pressure Used standard default settings**.** *1013.25* Site pressure [mb] *0* Altitude – at ground [km] *0* Height – above ground [km]	**Card 10a: Tilt albedo** **Tilted surface & local albedo (predominate within r = 100 m)** Standard Default is for a tilted panel 37^{o} from horizontal. Selected tilt [deg] = **0** and azimuth [deg] = **0** Selected vegetation: ***Grazing field (unfertilised)***
Card 3: Atmosphere * For PAR spectra used appropriate latitude-specific atmosphere. * For daily and annual irradiance selected: ***U.S. Standard Atmosphere*** * The effect of the difference between using the default U.S. standard atmosphere and latitude-specific atmosphere is < 0.2% on PAR total.	**Card 11: Spectral range** Selected spectral range: minimum **400** nm: maximum **700** nm Standard default solar constant [W m^{-2}]: 1,336.1 Standard default solar distance correction factor: 1.0
Card 4: Water vapour Used standard default setting: ***Calculate from reference atmosphere and altitude*** * This option automatically uses the settings specific for the atmosphere chosen on Card #3.	**Card 12: Output** Output File options: ***create .OUT and .EXT files include spectral results in both files*** Spectral range to be printed [nm]: minimum **400** nm: maximum **700** nm: interval (step) ***1*** Spectral results: Results in W m^{-2} (PAR) □ ***Direct normal irradiance*** □ ***Diffuse horizontal irradiance*** □ ***Global horizontal irradiance*** Results in umol m^{-2} s^{-1} (PPFD) □ ***Global horizontal photosynthetic photon flux*** □ ***Direct normal photosynthetic photon flux*** □ ***Diffuse horizontal photosynthetic photon flux***
Card 5: Columnar ozone abundance Used standard default setting: ***Use default from reference atmosphere***	**Card 13: Circumsolar** Circumsolar calculations Used standard setting: ***Bypass***
Card 6: Gaseous absorption and pollution used standard default setting: ***use defaults from selected atmosphere***	**Card 14: Smoothing** Extra scanning/smoothing Used standard setting: ***Bypass***
Card 7: Carbon dioxide Warning: Default value is out-of-date. Used an estimated 2009 CE value of **389** (ppmv) (NOAA Earth System Research Laboratory).	**Card 15: Illuminance** Extra illuminance and photosynthetically active radiation calculations Used standard setting: ***Bypass***
Card 7a: Extraterrestrial spectrum Used standard default setting: ***Gueymard 2004***	**Card 16: UV** Extra UV calculations Used standard setting: ***Bypass***
Card 8: Aerosol model Used standard default setting: Shettle & Fenn category: ***Rural***	**Card 17: Solar geometry** **Solar position and air mass** * Two configurations used (some settings override Cards 1-16) Configuration #1 Selected: ***Input elevation and azimuth angles*** **[deg]** Two runs needed. Record numbers 1-60 and 61-90. Apparent elevation angles (deg): **0-90** and azimuth angle (deg): **180** Configuration #2 Selected: ***Input year, month, day, hour, latitude, longitude, and time zone*** Specified year, month, day, hour and latitude of interest. For the purposes of the present study the longitude was set at long.: ***0*** and time zone: ***0***
Card 9: Atmospheric turbidity Used standard default turbidity: *0.084* Specified as: Default value: ***Aerosol optical depth at 500 nm***	

Supplementary figures

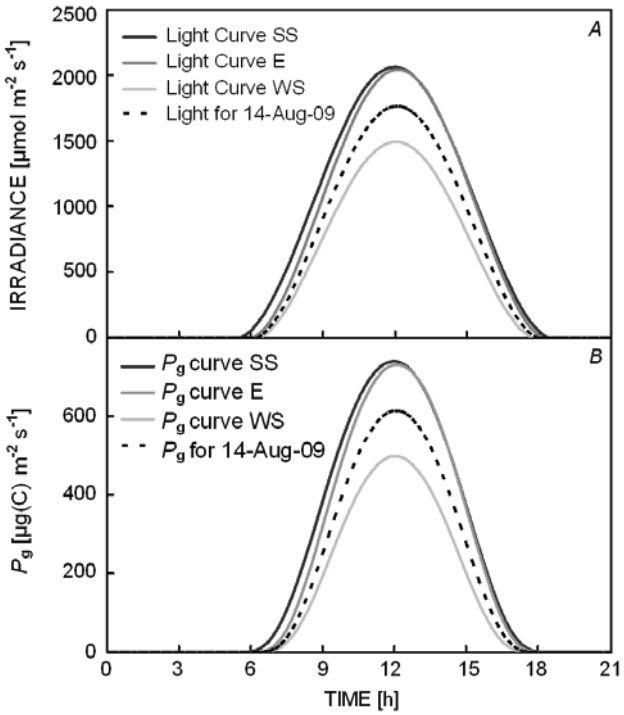

Fig. 1S. *A*: The diurnal irradiance patterns are quite different in tropical locations because the sun passes directly overhead twice a year. Light curves for Darwin, NT, Australia (latitude 12°28' S) for the summer and winter solstices, and the equinoxes and at an arbitrary date of 14-Aug-2009. There is little variation in the day-length over the year. The maximum noon PPFD is 2,152 µmol m^{-2} s^{-1} (59.9 mol m^{-2} d^{-1}) at the summer (wet-season) solstice (21-Dec-2009) and falls to 1,759 µmol m^{-2} s^{-1} (43.4 mol m^{-2} d^{-1}) for the winter (dry-season) solstice (21-Jun-2009). *B*: the estimated gross photosynthesis (P_g) (Eq. 7).

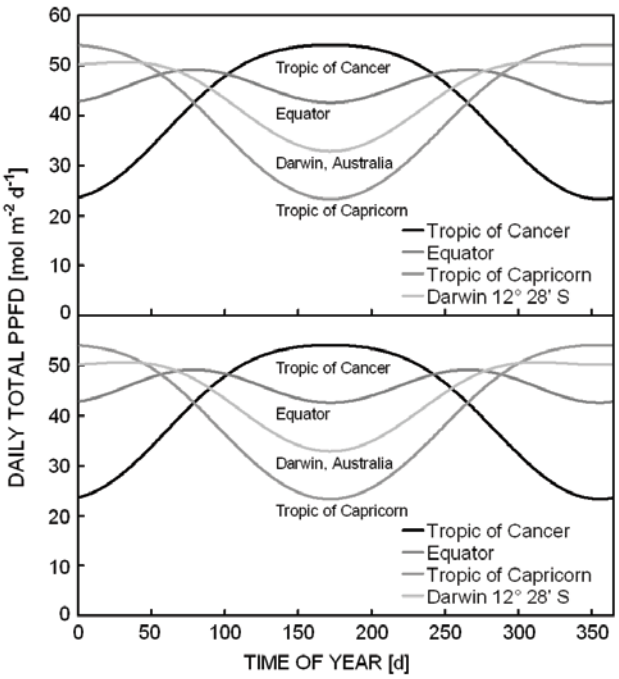

Fig. 2S. *A*: Daily irradiances for the tropics of Cancer and Capricorn, the equator and for Darwin, NT, Australia (latitude 12°28' S). The curves are similar for those found in mid-latitudes for the tropics of Cancer and Capricorn but at the equator maximum irradiance occurs twice a year at the equinoxes and is least when the sun is directly over the tropics of Cancer and Capricorn. *B*: The estimated diurnal gross photosynthesis (P_g) (Eq. 7).